AEA FUS 260

AEA Technology
Fusion
(UKAEA/Euratom Fusion Association)

Computation of a Model for the Sawtooth Crash

C G Gimblett and R J Hastie

February 1994

AEA Technology
Fusion

Culham, Abingdon
Oxfordshire OX14 3DB
United Kingdom
Telephone 0235 463311
Facsimile 0235 463647

Computation of a Model for the Sawtooth Crash

C G Gimblett and R J Hastie

AEA Technology, Fusion, Culham, Abingdon, Oxon, OX14 3DB, U.K.
(Euratom/UKAEA Fusion Association)

Abstract
A model for the sawtooth collapse, based on Taylor relaxation of the plasma core in a Tokamak, is described. The relaxation is assumed to take place within a central zone determined by the instability of localised resistive interchange modes, and is accompanied by an ideal MHD adjustment of the external region so as to maintain force balance across the interface. Using an aspect ratio expansion, equations determining the post-crash equilibrium are derived and solved in terms of equilibrium quantities prior to collapse. The crash model contains no arbitrary parameters. This model has been installed in the '1-1/2 D' resistive evolution code LARS, and in the paper we carry out a quantitative comparison of the simulation results with experimental data, in particular with the TEXTOR tokamak where detailed measurements are readily available.

1 Introduction

Many aspects of sawtooth phenomena in Tokamaks remain mysterious. It is important to be able to model the sawtooth instability as it has effects on ignition criteria in reactors, as well as on the confinement of fusion products. It is not known what controls the triggering of the rapid temperature collapse, and hence what determines the sawtooth period. The physical processes that take place during the abrupt ($\sim 100\mu s$ in JET) crash phase are also unknown. The earliest suggestions of Kadomtsev [1], [2] that the observed temperature collapse may simply be a consequence of a global $m = 1, n = 1$ flux reconnection in the plasma core were vitiated when detailed analysis of soft X-ray signals [3], [4] suggested that a sudden interruption of the relatively slow m=1 reconnection occurs when the magnetic island is of modest size ($W \sim r_1/3$ where W is the island width and r_1 the radius of the $q = 1$ magnetic surface). More evidence conflicting with the Kadomtsev reconnection model appeared when careful Faraday rotation measurements [5], [6] revealed that the value of the safety factor q remained below unity after the thermal crash of the sawtooth cycle. Further, the Kadomtsev model is associated with a time scale that is too slow to explain the crash phase in modern large tokamaks such as JET [7].

In this note we present results from an alternative model, based on fine scale reconnection in the plasma core. (We do not address here the problem of the interruption of the reconnection ('partial sawteeth') or the question of the triggering mechanism [8]).

A particularly well diagnosed experiment for this purpose is the TEXTOR tokamak [9], [10].

1.1 Description of the crash model.

The concept of Taylor relaxation [11] (minimisation of magnetic energy subject to a single topological constraint) has been successfully applied in the past to the Reversed Field Pinch [12]. In these devices the average curvature is always destabilising and because of the high magnetic shear there are many low-order mode rational surfaces within the plasma. Accordingly the Pinch has many degrees of freedom available to access the Taylor state. In the Tokamak there are typically only a few active mode rational surfaces and local resistive interchanges are generally stable. However, as the axial value of the safety factor q_0 drops below one, the average curvature as described by the quantity D_R [13],[14], [15] becomes unfavourable in an inner core and it is this region we might expect to Taylor relax. Accordingly we take the radius r_m within which Taylor relaxation occurs to be determined from $D_R(r_m) = 0$. We then seek solutions for the Taylor state ($\nabla \wedge \mathbf{B} = \mu \mathbf{B}, \mu$ constant) in this region (see [16] for an earlier investigation). In general this will now give rise to a force imbalance across r_m, and the plasma is allowed an ideal adiabatic displacement to restore equilibrium. In fact in the Tokamak ordering the imbalance is $O(\epsilon^2)$ and the toroidal field in the external region changes to accommodate it. We further assume that viscous forces are sufficient to convert (via dissipation of plasma kinetic energy) all the energy lost during the relaxation into thermal plasma energy. So the model concerns four constraints; core helicity and toroidal flux, total energy, and force balance at r_m. Analytic expressions for these quantities in the relaxed state can be obtained using the aspect ratio expansion limit employed by the '1-1/2 D' resistive evolution code LARS [17]. Computing these quantities numerically for the pre-crash state then allows the post-crash state to be completely defined simply by equating pre- and post-crash values. In Section 2 we derive the equations describing the post-crash equilibrium, and the constraint equations which determine the relevant constants. In Section 3 we obtain explicit solutions for these equations and examine the energetics of the process. It is well known experimentally [18] that the sawtooth oscillation is invariably associated with $m = 1$ (m is the poloidal mode number) activity and in Section 4 we outline the rôle that this mode plays in our model, together with a discussion of the D_R criterion in more detail. Section 5 briefly describes the installation of the crash model in the LARS evolution code, and finally in Section 6 we give results obtained by the code when applied to simulating sawteeth in the TEXTOR tokamak.

2 The Post-crash Equilibrium

Following [19] we transform from the usual cylindrical co-ordinate system (R, ϕ, Z) based on the axis of toroidal symmetry to a system (r, θ, ϕ) where magnetic surfaces have constant r and θ is a poloidal angle, and consider a large aspect ratio, $\beta \sim O(\epsilon^2)$ model of a Tokamak equilibrium, with the magnetic field given by

$$\mathbf{B} \;=\; R_0 B_0 [g(r) \nabla \phi + f(r) \nabla \phi \wedge \nabla r]. \quad (1)$$

The relaxation process is subject to the dual constraints of helicity conservation

$$K \;=\; \int_{core} \mathbf{A}.\mathbf{B} d\tau = constant, \quad (2)$$

and toroidal flux conservation

$$\Phi \;=\; \int_0^{r_m} r g(r) dr = constant. \quad (3)$$

In the final post-crash state the equilibrium has two distinct zones. Within the core ($r < r_m$) the plasma is in a Taylor relaxed state defined by $\mathbf{J} = \mu\mathbf{B}, p = \bar{p}$ with μ and $\bar{p}$ (the plasma pressure) constant. It follows that the poloidal and toroidal field functions $f(r), g(r)$ are related by

$$\mu f \;=\; -g'. \quad (4)$$

Hence following reference [20] and expanding the inverse Grad-Shafranov equation [19] in powers of inverse aspect ratio ϵ, so that

$$f \;=\; \epsilon f_1(r) + \epsilon^3 f_3(r) + \cdots, \quad (5)$$
$$g \;=\; 1 + \epsilon^2 g_2(r) + \cdots, \quad (6)$$
$$p \;=\; \epsilon^2 p_2(r) + \cdots \quad (7)$$

and writing $\mu = \epsilon\mu_1 + \epsilon^3\mu_3 + \cdots$ we obtain

$$f_1 \;=\; \frac{1}{2}\mu_1 r, \quad (8)$$
$$g_2 \;=\; -\frac{1}{4}\mu_1^2 r^2 + \bar{g}_2, \quad (9)$$
$$p_2 \;=\; \bar{p}_2, \quad (10)$$

with $\bar{p}_2$ and $\bar{g}_2$ constants. We seek a solution for the equilibrium flux surfaces in the form

$$R \;=\; R_0 - \epsilon r cos(\theta) - \epsilon^2\Delta(r) + \epsilon^2(E(r)cos(\theta) + T(r)cos(2\theta)) + \cdots$$
$$Z \;=\; \epsilon r sin(\theta) + \epsilon^2(E(r)sin(\theta) + T(r)sin(2\theta)) + \cdots, \quad (11)$$

where Δ is the equilibrium (Shafranov) shift of the surfaces and E, T represent the externally imposed ellipticity and triangularity. Inserting (11) into the inverse Grad-Shafranov we find that these shaping functions satisfy

$$\begin{aligned}
\Delta'' + (\frac{2(rf_1)'}{rf_1} - \frac{1}{r})\Delta' - \frac{1}{R_0} + \frac{2rp_2'}{R_0 f_1^2 B_0^2} &= 0, \\
E'' + (\frac{2(rf_1)'}{rf_1} - \frac{1}{r})E' - 3\frac{E}{r^2} &= 0, \\
T'' + (\frac{2(rf_1)'}{rf_1} - \frac{1}{r})T' - 8\frac{T}{r^2} &= 0
\end{aligned} \quad (12)$$

Using eqns.(8) and (10) in (12) we easily find that in the core region

$$\begin{aligned}
\Delta(r) &= \Delta_0 + \frac{1}{8}\frac{r^2}{R_0}, \\
E(r) &= \bar{E}\frac{r}{r_m}, \\
T(r) &= \bar{T}(\frac{r}{r_m})^2,
\end{aligned} \quad (13)$$

where $\Delta_0, \bar{E}$ and $\bar{T}$ are constants, to be determined by matching to outer solutions at $r = r_m$.

The latter expressions are only required if we choose to obtain a solution for $f_3(r)$. We will, however, determine f_3 because f_3 and g_2 both contribute to the departure of the $q(r)$ profile from constancy, and this departure may be of considerable importance for the subsequent evolution and $m = 1$ stability of the equilibrium.

Employing eqns.(8 - 13) we obtain $f_3(r)$ from the higher order pressure balance equation (see [20]) as

$$\begin{aligned}
f_3(r) = &\frac{1}{2}\mu_3 r - \frac{1}{2}\mu_1 r(\frac{\Delta_0}{R_0} - \bar{g}_2) - \frac{1}{16}\mu_1^3 r^3 \\
&-\frac{29}{64}\frac{\mu_1 r^3}{R_0^2} - \frac{\mu_1 r}{r_m^2}(\bar{E}^2 + 3\bar{T}^2(\frac{r}{r_m})^2).
\end{aligned} \quad (14)$$

Turning now to the plasma in the outer region $[r_m, a]$, we require that this plasma behaves in an ideal (flux-conserving) manner under compression/expansion as the initial mixing radius, which we denote by r_{mi}, is displaced to r_m with

$$r_m = r_{mi} + \xi(r_{mi}). \quad (15)$$

Throughout this ideal region we write

$$r = r_i + \xi(r_i), \tag{16}$$

and require local flux conservation

$$\hat{g} r dr = g r_i dr_i, \tag{17}$$
$$\hat{f} dr = f dr_i, \tag{18}$$

and constancy of entropy

$$[\hat{p}(r)]^{\frac{1}{\gamma}} r dr = [p(r_i)]^{\frac{1}{\gamma}} r_i dr_i, \tag{19}$$

where $\hat{g}(r)$, $\hat{f}(r)$ and $\hat{p}(r)$ are the equilibrium fields and pressure in the outer region in the final post-crash state. From eqns.(16 - 19) it follows that

$$\hat{p} = p[1 - \frac{1}{r_i}\frac{d}{dr_i}(r_i\xi(r_i))]^{\gamma}, \tag{20}$$
$$\hat{g} = g[1 - \frac{1}{r_i}\frac{d}{dr_i}(r_i\xi(r_i))], \tag{21}$$
$$\hat{f} = f[1 - \frac{d\xi(r_i)}{dr_i}]. \tag{22}$$

Inserting these expressions into the pressure balance relation in the outer region

$$\frac{\mu_0}{B_0^2}\frac{d\hat{p}_2}{dr} + \frac{d\hat{g}_2}{dr} + \frac{\hat{f}_1}{r}\frac{d}{dr}(r\hat{f}_1) = 0, \tag{23}$$

and noting that the dominant role played by the toroidal magnetic field requires $\xi(r_i)/r_i \sim O(\epsilon^2)$ we obtain,

$$\frac{\mu_0}{B_0^2}\frac{dp_2}{dr_i} + \frac{d}{dr_i}[g_2 - \frac{1}{r_i}\frac{d}{dr_i}(r_i\xi)] + \frac{f_1}{r_i}\frac{d}{dr_i}(r_i f_1) = 0, \tag{24}$$

and hence

$$\frac{d}{dr_i}[\frac{1}{r_i}\frac{d}{dr_i}(r_i\xi(r_i))] = 0, \tag{25}$$

with solution

$$\xi(r) = \frac{r_m}{r}\frac{(a^2-r^2)}{(a^2-r_m^2)}\xi(r_m). \tag{26}$$

In deriving eqn.(26) we have assumed a conducting wall at the plasma boundary $r = a$.

Equation (26) completes the solution for the pressure and magnetic fields $\hat{p}_2(r), \hat{g}_2(r), \hat{f}_1(r)$ in the outer region. However, the post-crash equilibrium contains the four undetermined constants ($\mu_1, \bar{p}_2, \bar{g}_2$, and $\xi(r_m)$) in the leading order quantities ($p_2(r), g_2(r), f_1(r)$), and contains further undetermined constants ($\Delta_0, \bar{E}, \bar{T}$ and μ_3) if we extend the equilibrium description to include $f_3(r)$ which, as discussed above, we wish to do.

To determine these constants we return to the four constraints discussed in the introduction. These are conservation of (i) Core helicity K, (ii) Core toroidal flux Φ, and (iii) Total energy W together with pressure balance across the mixing radius r_m.

2.1 Conservation of Core Helicity K

Taking the magnetic field in the form (1) the normalised core helicity may be written

$$\begin{aligned} K &= \int_0^{r_m} f(r)dr \int_0^r r'g(r')dr' - \int_0^{r_m} rg(r)dr \int_{r_m}^r f(r')dr' \\ &= 2\int_0^{r_m} f(r)dr \int_0^r r'g(r')dr'. \end{aligned} \tag{27}$$

(The integration limits in (27) are chosen to eliminate contributions to K from fields exterior to the core [21]). Hence writing $K = \epsilon K_1 + \epsilon^3 K_3 + \cdots$, and denoting quantities in the initial state (prior to collapse) by a subscript i, and those in the final (post-crash) state by a subscript f, we obtain

$$K_{1i} = \int_0^{r_{mi}} f_{1i}(r)r^2dr. \tag{28}$$

The value of K_1 in the post-collapse state is easily calculated using eqn.(8). Thus employing helicity conservation we obtain

$$K_{1i} = \frac{1}{8}\mu_1 r_{mi}^4. \tag{29}$$

We will return to the $O(\epsilon^3)$ contributions to this constraint relation later, but it is convenient to derive the other constraint equations in leading order before returning to the discussion of K_{3f} and K_{3i}.

2.2 Toroidal Flux Conservation

Making use of the definitions

$$\begin{aligned} \Phi_i &= \int_0^{r_{mi}} r g_i(r) dr, & (30) \\ \Phi_f &= \int_0^{r_m} r[1 - \frac{1}{4}\mu_1^2 r^2 + \bar{g}_2 + O(\epsilon^4)]dr, \text{and} & (31) \\ r_m &= r_{mi} + \xi(r_{mi}) & (32) \end{aligned}$$

we find flux conservation in zero order provided $\xi(r_{mi})/r_{mi} \sim O(\epsilon^2)$. Then in ϵ^2 order we obtain

$$\begin{aligned} \Phi_{i2} &= \int_0^{r_{mi}} r g_{2i}(r) dr, \\ &= r_{mi}\xi(r_{mi}) - \frac{1}{16}\mu_1^2 r_{mi}^4 + \frac{1}{2}\bar{g}_2 r_{mi}^2. & (33) \end{aligned}$$

where the distinction between r_m and r_{mi} can be neglected on the right hand side, since it is an $O(\epsilon^2)$ correction.

2.3 Global Energy Conservation

Writing this correct to $O(\epsilon^2)$ we obtain

$$\begin{aligned} W_i &\propto \int_0^a r[\frac{3}{2}p_2 + \frac{B_0^2}{2\mu_0}(1 + f_1^2 + 2g_2)]dr + O(\epsilon^4), & (34) \\ W_f &\propto \int_0^{r_m} r[\frac{3}{2}\bar{p}_2 + \frac{B_0^2}{2\mu_0}(1 + 2g_{2f} + \frac{1}{4}\mu_1^2 r^2)]dr \\ &+ \int_{r_m}^a r[\frac{3}{2}\hat{p}_2 + \frac{B_0^2}{2\mu_0}(1 + 2\hat{g}_2 + \hat{f}_1^2)]dr & (35) \end{aligned}$$

As in the case of toroidal flux conservation, energy conservation in leading order, $O(\epsilon^0)$, is automatic. Toroidal flux conservation ensures that the toroidal field energy is also conserved in $O(\epsilon^2)$. Finally, anticipating the fact that $\xi(r)$ will be $O(\epsilon^2)$ in the outer region, and therefore that the adiabatic compression of p and compression of the poloidal flux will have a negligible effect on $\hat{p}_2$ and $\hat{f}_1$, we use the results

$$\hat{f}_1 \simeq f_{1i}(r), \tag{36}$$

$$\hat{p}_2 \simeq p_{2i}(r) \tag{37}$$

to write energy conservation in the form

$$\int_0^{r_m} r[\frac{3}{2}p_2 + \frac{B_0^2}{2\mu_0}f_1^2]dr = \frac{3}{4}\bar{p}_2 r_m^2 + \frac{B_0^2}{32\mu_0}\mu_1^2 r_m^4 \tag{38}$$

where, once again, the distinction between r_m and r_{mi} need not be retained.

2.4 Pressure Balance at the Mixing Radius r_m

Equilibrium at the mixing radius demands continuity of the total pressure $(p + \frac{B^2}{2\mu_0})$. Thus we require

$$\hat{p}_2(r_m) + \frac{B_0^2}{2\mu_0}(1 + 2\hat{g}_2 + \hat{f}_1^2) = \bar{p}_2 + \frac{B_0^2}{2\mu_0}(1 + 2\bar{g}_2 - \frac{1}{4}\mu_1^2 r_m^2). \tag{39}$$

Although the small $O(\epsilon^2)$ displacement of the mixing radius has a negligible effect on pressure and poloidal magnetic field, it must be taken into account when calculating the toroidal magnetic field $\hat{g}_2$. Thus using eqns.(21) and (26) we find

$$\hat{g}_2 = g_{2i} + \frac{2r_m\xi(r_m)}{(a^2 - r_m^2)}. \tag{40}$$

Introducing this into (39) we obtain

$$\begin{aligned} \frac{\mu_0\bar{p}_2}{B_0^2} + \bar{g}_2 - \frac{1}{8}\mu_1^2 r_m^2 - \frac{2r_m\xi(r_m)}{(a^2 - r_m^2)} &= \frac{\mu_0 p_2(r_m)}{B_0^2} + \frac{1}{2}f_1^2(r_m) + g_2(r_m), \\ &\equiv \hat{P}_2. \end{aligned} \tag{41}$$

The four eqns.(29), (33), (38) and (41) can now be solved for the parameters $\bar{p}_2, \mu_1, \bar{g}_2$ and $\xi(r_m)$ in terms of which the post-collapse equilibrium is specified in leading order. Before solving these equations we return to the determination of f_3, and hence of the parameters $\mu_3, \Delta_0, \bar{E}$, and $\bar{T}$ which remain to be calculated. The three quantities $\bar{E}, \bar{T}$ and Δ_0 which describe the shape and toroidal shift of the magnetic surfaces in the plasma core are simply obtained by matching at the mixing radius to the corresponding quantities in the outer region.

Since in the outer region $\hat{p}_2(r) = p_{2i}(r)$ and $\hat{f}_1 = f_{1i}(r)$ it follows that $\Delta(r), E(r)$ and $T(r)$ satisfy the same differential equations (12) as in the initial equilibrium. However, because a new boundary condition (matching to solutions at r_m) must now be applied, the solutions differ from those in the initial state. Thus surface shapes and the toroidal shift in the outer region are modified by the relaxation event in the core. The appropriate boundary condition at $r = r_m$ is obtained by integrating the equilibrium shaping and Shafranov shift equations across the mixing radius to obtain the jump conditions

$$\begin{aligned} [E' f_1^2] &= [T' f_1^2] = 0, \\ [\Delta' f_1^2] &= \frac{2r_m}{R_0 \mu_0 B_0^2}(\bar{p}_2 - p_i(r_m)), \end{aligned} \tag{42}$$

where

$$[A] \equiv \lim_{\delta \to 0}[A(r_m + \delta) - A(r_m - \delta)]. \tag{43}$$

The above relations ensure that the Grad-Shafranov equilibrium equation is satisfied at $r = r_m$ in first order. Then, matching E, T and Δ at $r = r_m$, we find the boundary conditions appropriate to the outer region solutions are

$$\begin{aligned} \frac{\hat{E}'}{\hat{E}}(r_m + \delta) &= \frac{1}{4}\frac{\mu_1^2 r_m}{f_{1i}^2(r_m)}, \\ \frac{\hat{T}'}{\hat{T}}(r_m + \delta) &= \frac{1}{2}\frac{\mu_1^2 r_m}{f_{1i}^2(r_m)}, \\ \hat{\Delta}'(r_m + \delta) &= \frac{1}{16}\frac{\mu_1^2 r_m^3}{R_0 f_{1i}^2(r_m)} + \frac{2r_m}{R_0 \mu_0 B_0^2 f_1^2}(\bar{p}_2 - p_i(r_m)). \end{aligned} \tag{44}$$

and that the constants $\bar{E}$, $\bar{T}$ and Δ_0 are then given by

$$\bar{E} = \hat{E}(r_m), \tag{45}$$

$$\bar{T} = \hat{T}(r_m), \tag{46}$$

$$\Delta_0 = \hat{\Delta}(r_m) - \frac{1}{8}\frac{r_m^2}{R_0^2}, \tag{47}$$

where $\hat{E}$, $\hat{T}$ and $\hat{\Delta}$ represent the outer region solutions in the post-crash equilibrium.

To determine μ_3 we require helicity conservation in ϵ^3 order. Thus

$$K_{3i} = \int_0^{r_{mi}} r^2 f_3 dr + 2\int_0^{r_{mi}} f_1 dr \int_0^{r} r' g_2(r')dr' \qquad (48)$$

must be equated to K_{3f}. Making use of eqns.(8), (9) and (14) and recalling that in evaluating K_{1f}

$$K_{1f} = \frac{1}{8}\mu_1 r_m^4 \qquad (49)$$

$$= \frac{1}{8}\mu_1 r_{mi}^4 (1 + \frac{4\xi(r_m)}{r_m}), \qquad (50)$$

we retained only the leading contribution in writing eqn.(29), we obtain the following expression for K_{3f}

$$K_{3f} = \frac{1}{8}\mu_1 r_m^4 [2\bar{g}_2 - \frac{\Delta_0}{R_0} + \frac{\mu_3}{\mu_1} + \frac{4\xi(r_m)}{r_m}]$$
$$-\frac{1}{48}\mu_1 r_m^4 [\mu_1^2 r_m^2 + \frac{29}{8}\frac{r_m^2}{R_0^2}]$$
$$-\frac{1}{4}\mu_1 r_m^2 [\bar{E}^2 + 2\bar{T}^2]. \qquad (51)$$

Now making use of eqns.(45)-(47) and helicity conservation in ϵ^3 order

$$K_{3i} = K_{3f}, \qquad (52)$$

μ_3 is determined and a complete solution for f_3 in the plasma core can be obtained.

3 Solution of the Constraint Equations

In this Section we complete the calculation of the post-crash equilibrium by solving eqns.(29), (33), (38), (41) and (52) for the constants $\mu_1, \bar{p}_2, \bar{g}_2, \xi(r_m)$ and μ_3.

It is convenient to first define the following dimensionless quantities which can be calculated from a knowledge of the equilibrium immediately prior to the sawtooth crash

$$\hat{K}_1 = \frac{2}{r_{mi}^3}\int_0^{r_{mi}} r^2 f_1(r)dr, \tag{53}$$

$$\hat{\Phi}_2 = \frac{2}{r_{mi}^2}\int_0^{r_{mi}} r g_2(r)dr, \tag{54}$$

$$\hat{W}_2 = \frac{2}{r_{mi}^2}\int_0^{r_{mi}} r[\frac{3\mu_0 p_2(r)}{2B_0^2} + \frac{1}{2}f_1^2(r)]dr, \tag{55}$$

$$\hat{P}_2 = \frac{\mu_0 p_2(r_{mi})}{B_0^2} + \frac{1}{2}f_1^2(r_{mi}) + g_2(r_{mi}), \tag{56}$$

$$\hat{K}_3 = \frac{2}{r_{mi}^3}K_{3i}. \tag{57}$$

Having evaluated these five initial quantities the relevant constraint equations take the form

$$4\hat{K}_1 = \mu_1 r_m, \tag{58}$$

$$\hat{\Phi}_2 = \bar{g}_2 + 2\frac{\xi(r_m)}{r_m} - \frac{1}{8}\mu_1^2 r_m^2, \tag{59}$$

$$\hat{W}_2 = \frac{3}{2}\frac{\mu_0\bar{p}_2}{B_0^2} + \frac{1}{16}\mu_1^2 r_m^2, \tag{60}$$

$$\hat{P}_2 = \frac{\mu_0\bar{p}_2}{B_0^2} + \bar{g}_2 - \frac{1}{8}\mu_1^2 r_m^2 - \frac{2r_m\xi(r_m)}{(a^2 - r_m^2)}, \tag{61}$$

$$\begin{aligned} 4\hat{K}_3 = {} & \mu_1 r_m[2\bar{g}_2 + \frac{\mu_3}{\mu_1} + \frac{4\xi(r_m)}{r_m} - \frac{\Delta(r_m)}{R_0}] \\ & -\mu_1 r_m[\frac{\mu_1^2 r_m^2}{6} + \frac{23}{48}\frac{r_m^2}{R_0^2} + \frac{2E^2(r_m)}{r_m^2} + \frac{4T^2(r_m)}{r_m^2}]. \end{aligned} \tag{62}$$

Hence, solving, we find

$$\mu_1 r_m = 4\hat{K}_1, \tag{63}$$

$$\frac{\mu_0\bar{p}_2}{B_0^2} = \frac{2}{3}[\hat{W}_2 - \hat{K}_1^2], \tag{64}$$

$$\frac{\xi(r_m)}{r_m} = \frac{1}{2}[1 - \frac{r_m^2}{a^2}][\hat{\Phi}_2 - \hat{P}_2 + \frac{2}{3}(\hat{W}_2 - \hat{K}_1^2)], \tag{65}$$

$$\bar{g}_2 = \hat{\Phi}_2 + 2\hat{K}_1^2 - [1 - \frac{r_m^2}{a^2}][\hat{\Phi}_2 - \hat{P}_2 + \frac{2}{3}(\hat{W}_2 - \hat{K}_1^2)], \quad (66)$$

$$\mu_3 r_m = \hat{K}_1[4\frac{\Delta(r_m)}{R_0} + 8\frac{E^2(r_m)}{r_m^2} + 16\frac{T^2(r_m)}{r_m^2} + \frac{23}{12}\frac{r_m^2}{R_0^2} - 8\hat{\Phi}_2] + 4\hat{K}_3 + \frac{80}{3}\hat{K}_1^3. \quad (67)$$

3.1 An Analytic Example

As an example we calculate the value of the safety factor on axis, q_0, in the post-crash equilibrium as a function of the initial state parameters.

For this we consider an initial current profile of the form used by Kadomtsev [2]

$$j = j_0(1 - \frac{r^2}{a^2}), \quad (68)$$

corresponding to a $q(r)$ profile of the form

$$\frac{1}{q} = \frac{1}{q_0}(1 - \frac{r^2}{2a^2}). \quad (69)$$

Now writing K_{1i} in the form

$$K_{1i} = \int_0^{r_{mi}} \frac{r^3 dr}{q(r)}, \quad (70)$$

we find

$$K_{1i} = \frac{r_{mi}^4}{4q_0}[1 - \frac{2}{3}(1 - q_0)\frac{r_{mi}^2}{r_1^2}], \quad (71)$$

where $q(r_1) \equiv 1$. Equating this to the value of the helicity (in the cylindrical limit) in the post-crash equilibrium

$$K_{1f} = \frac{r_{mi}^4}{4q_f} \quad (72)$$

determines the value of q_f in the core after relaxation

$$q_f = q_0[1 - \frac{2}{3}(1 - q_0)\frac{r_m^2}{r_1^2}]^{-1}. \quad (73)$$

Clearly this remains below unity if

$$\frac{r_m}{r_1} < \sqrt{\frac{3}{2}} \tag{74}$$

and in particular, if $r_m/r_1 \simeq 1$ we find

$$(1-q_f) = \frac{1}{3}(1-q_0)[1-\frac{2}{3}(1-q_0)]^{-1}. \tag{75}$$

So, for example, an initial value of axial q, $q_0 = 0.75$ results in a final value $q_f = 0.9$. Figure 1 gives a plot of $q(0)$ after the crash against that before it for various values of r_m/r_1.

3.2 Energy Accounting

We now consider how energy is distributed after the sawtooth crash. The relaxation process reduces the magnetic energy in the plasma core. Inspection of eqn.(38) shows that the loss of poloidal field energy in the core,

$$\Delta W_\theta = \frac{B_0^2}{2}\int_0^{r_m} r[f_{1f}^2 - f_{1i}^2]dr, \tag{76}$$

is exactly compensated by the gain in core thermal energy $\Delta W_p = -\Delta W_\theta$ with

$$\Delta W_p = \frac{3}{2}\int_0^{r_m} r[p_f - p_i]dr. \tag{77}$$

The energy in the toroidal magnetic field in the core decreases if the displacement ξ is positive (expansion of the core plasma), but is exactly compensated (up to $O(\epsilon^2)$) by the increase in toroidal field energy in the outer (compressed) region.

4 The D_R criterion and the rôle of the $m = 1$ mode

As alluded to in Section 1.1, there are two primary difficulties that arise when seeking to base a sawtooth model on the D_R condition. The first is that (as is the case for the simulations described in Section 6), the average curvature is unfavourable in the core *during* the ramp and the crash does not occur when D_R changes sign. The second is that the sawtooth oscillation is invariably associated with $m = 1$ activity, hitherto not mentioned. In this Section we briefly show how these observations can be accommodated within the model (full details will be given in a future paper).

4.1 The D_R stability criterion revisited

The criterion for localised resistive 'g' modes of tearing parity was first given in Ref. [13]. The dispersion relation found was

$$\Delta' = \frac{2.1}{s^{1/2}}\left(\frac{S}{n^2}\right)^{3/4}\hat{\gamma}^{5/4}\left[1-\frac{\pi}{4}\frac{sD_R}{\hat{\gamma}^{3/2}}\left(\frac{n^2}{S}\right)^{1/2}\right], \tag{78}$$

where $s = rq'/q$ is the magnetic shear, n the toroidal mode number, $S = (\tau_\eta/\tau_A)$ is the Lundquist number with τ_A, τ_η being the Alfvén and resistive timescales respectively.

The original motivation behind deriving eqn.(78) was to investigate the toroidal stabilising effect of favourable curvature ($D_R < 0$) on the global tearing mode. In fact the authors found, using (78), that the conventional cylindrical instability criterion $\Delta' > 0$ was replaced by

$$\Delta' > \Delta'_c = \frac{1.52}{s^{1/2}}\left[-sD_R\right]^{5/6}\left(\frac{S}{n^2}\right)^{1/3}. \tag{79}$$

We now wish to investigate the *opposite* case and consider the effect of a stable tearing mode index ($\Delta' < 0$) in the presence of unfavourable average curvature. In our region of interest $q_0 < q < 1$ the relevant resonant surfaces ($q = m/n$) have high (m, n) e.g. (9,10), (10,11) *etc.* and hence the associated tearing mode indices are stable with Δ' well approximated by $-2m \sim -2n$. For this case eqn.(78) now gives

$$(-\Delta') < \frac{2.74}{s^{1/2}}\left[sD_R\right]^{5/6}\left(\frac{S}{n^2}\right)^{1/3}. \tag{80}$$

as the instability criterion. If we estimate the numbers in eqn.(80) for typical smooth current and pressure profiles we find that the stabilising effect of the outer region ($\Delta' < 0$) outweighs the destabilising effect of adverse curvature ($D_R > 0$) for $n \sim 0.1S^{1/5}$ and greater. For present day devices this gives $n \sim 5$, and so we find that the relevant, tearing parity 'g' modes are indeed stable. Although twisting parity 'g' modes do not experience the stabilising effect of negative Δ' they may be stabilised by compressible effects during the ramp phase. In the next sub-section we describe how the $m = 1$ mode can initiate the collapse of this stabilising effect.

4.2 The rôle of the $m = 1$ mode

We assume that at some stage in the ramp, the resistive $m/n = 1/1$ mode starts to grow at $r = r_1$. The (rotating) magnetic island produced by the mode is responsible for the pre-cursor oscillations often observed [18]. Now the island generates a sharp increase in the pressure gradient $p'(r)$ just outside the island separatrix [22]. In the first instance these localised pressure gradients are both in regions of stable D_R as $D_R < 0$ for $r_m < r < r_1$ (see Section 6 below), and a period of 'benign' $m = 1$ island growth occurs. Eventually the separatrix reaches r_m (an event that could be hastened by the bringing into co-rotation of the $m/n = 1/1$ and $2/1$ surfaces [23]). Large destabilising values of D_R are now generated by the locally steep pressure gradient close to the separatrix and the $m/n \sim 10/11$ tearing modes can grow rapidly; this propagates the pressure front inwards towards the axis, but not outwards of course because D_R is stabilising beyond $q \sim 1$. Thus the collapse process is intimately controlled by unfavourable curvature. The result is Taylor relaxation of the core $0 < r < r_m$, exactly of the sort modelled in Sections 2 and 3 above. We note that the $m = 1$ island structure is now free of the driving due to pressure and current gradients in the core and may undergo inverse reconnection, but we do not address this feature in the present model.

5 Implementation of the model in LARS

The LARS code is a '1-1/2 D' resistive evolution code for toroidal plasmas that employs flux-surface averaged equations evaluated as an expansion in inverse aspect ratio [17]. In implementing the crash model of this paper into LARS we must first dictate the criteria which have to be met for executing the crash. As explored in [23], a possible trigger mechanism for the crash is the bringing into co-rotation of the $q = 1$ and 2 surfaces by the electromagnetic torque due to the sideband of a dominant $m = 1$ mode. Simulation of this behaviour would require us to monitor the plasma momentum equation during a sawtooth ramp and, further, have a full knowledge of the plasma rotation profiles in the absence of instability. This facility is not available at present and we must have recourse to a heuristic model of the ramp time. An example would be the use of the ramp time scaling law of Park *et. al.* [24]. For illustrative purposes in the examples that follow we simply dictate a ramp time; the criterion for implementing a crash after a ramp time is then that D_R be below zero.

Once these criteria are met the quantities $\hat{K}_1 - \hat{K}_3$ of eqns.(53) - (57) are computed and used to solve for the associated quantities $\mu_1, \bar{p}_2$ *etc.* of eqns.(63) - (67) that determine the new Taylor relaxed core and mixing radius displacement. The new field and pressure profiles within this radius are then calculated (note that $g_2(r)$ has also to be calculated in the exterior region, see eqn.(40)). The next step is to solve over the whole radius for new shaping (ellipticity $E(r)$ and triangularity $T(r)$) and Shafranov shift $\Delta(r)$ profiles. As discussed in Sec. 2.4 this is achieved by first solving the relevant equations in $r_m < r < a$ subject to the boundary conditions of eqn.(44) at r_m ($E(a)$ and $T(a)$ are fixed given values while $\Delta(a) = 0$). These solutions then determine the constants $\bar{E}, \bar{T}$ and Δ_0 which give the inner relaxed solutions of eqns.(13). In practice, the Gaussian tri-diagonal solver employed in LARS can automatically accommodate the jump conditions and shaping and shift are solved for in one sweep. The plasma is now allowed to continue resistive evolution until the criteria for the next crash are met.

6 Simulation of sawteeth in the TEXTOR tokamak

The observation that $q(0)$ was below one and remained so throughout a sawtooth crash was first made on the TEXTOR Tokamak [9]. This finding cast some doubt on the reconnection model proposed by Kadomtsev [2] which predicted a return of $q(0)$ to one after the crash. Further, the TEXTOR team recently reported that the inversion radius r_{inv} (the radius at which the emissivity remained unperturbed) was significantly smaller than the radius of the $q = 1$ surface as inferred from polarimetric measurements ($r_{inv} = 13$ cm., $r_1 = 15.5$ cm., $a_0 =$ minor radius $= 42.5$ cm. We can expect our model to produce $r_m < r_1$ (and hence $r_{inv} < r_1$) for TEXTOR equilibria as can be seen by writing the expression for D_R [14] in the case of no externally applied shaping fields (for circular cross-section)

$$D_R = -\frac{2Rp'q^3}{rq'B_0^2}\left(\frac{q}{Rq'}(1-\frac{1}{q^2})+\Delta'\right), \quad (81)$$

So at r_1 we have

$$D_R = -\frac{2Rp'\Delta'}{r_1q'B_0^2}. \quad (82)$$

Orthodox cases at $q = 1$ produce $p' < 0, q' > 0, \Delta' > 0$ and therefore $D_R(r_1) > 0$. So if the criterion for instability $D_R < 0$ is met at r_m we will find that $r_m < r_1$. Indeed we have from [25] that

$$\Delta'(r_1) \sim -\frac{r}{R}(\beta_p(r_1) + l_i(r_1)/2) \quad (83)$$

$$\sim -\frac{r}{R}(\beta_p(r_1) + \frac{1}{4}) \quad (84)$$

where β_p and l_i are the plasma poloidal beta and internal inductance ($= 1/2$ assuming a flat current profile inside r_1). So expanding eqn.(81) about $q = 1$ gives

$$\frac{r_m - r_1}{r_1} \sim -\frac{1}{2}(\beta_p(r_1) + \frac{1}{4}). \quad (85)$$

The TEXTOR simulation that is described in the remainder of this Section gives

$$\frac{r_m/a - r_1/a}{r_1/a} = \frac{0.33 - 0.39}{0.39} = -0.154 \quad (86)$$

implying $\beta_p(r_1) \sim 0.05$. The main TEXTOR parameters chosen for the simulations were those reported in [9], [10] $a_0/R_0 = 42.5./176.0\text{cm.}, B_0 = 2.2\text{T.}, n_e(0) = 5.8\text{cm}^3 10^{13}, I_p = 380$ kA, and the thermal diffusivity chosen to give $< T(0) >\sim 0.9$ Kev. The sawtooth repetition time was taken from experiment to be 20 ms. Initial q and T profiles were then evolved using LARS (with the sawtooth model incorporated) until a quasi-steady state was achieved. The final state was in fact independent of the initial profiles chosen (provided $q(a)$ and hence I_p was held fixed). The resulting evolution of the axial q is shown in Fig. 2. In the quasi-steady state the simulation gave $< q(0) >= 0.76$ and $\delta q(0) = 0.08$ in excellent agreement with the experimentally observed $< q(0) >= 0.76$ and $\delta q(0) = 0.07$. The radial q profile at equally spaced times in the ramp period is shown in Fig. 3. Note that the effect of the sawtooth activity is to produce a mean electromotive force in the plasma core. Without sawtooth activity the axial q would evolve neo-classically down to ~ 0.45 for this simulation. The sawtooth activity in fact has the average effect of 'backing off' the externally applied voltage, reducing the axial current and increasing the q above it's neo-classical value. The sawtooth acts as an 'anti-dynamo'. To further demonstrate this a run was performed with the sawteeth suppressed until $t = 0.3$ sec. into the simulation at which point they were switched on. The resulting re-establishment of the quasi-steady state is shown in Fig. 4.

In Fig. 5 we reproduce the experimental observation of $T(0)- < T(0) >$ during a sawtooth ramp reported in [10]. Fig. 6 shows the result of the LARS simulation with (inset) the radial profiles of $T(r)$ at equally spaced times in the ramp. The position of the $q = 1$ surface is marked, and accords well with the observation in [10] that the $q = 1$ surface "appears to be close to the location with maximum inverted sawtooth amplitude and does not coincide with r_m". Table 1 gives a brief comparison of the LARS simulation with the TEXTOR observations.

Table 1	$< q(0) >$	$\delta q(0)$	r_1/a	r_{inv}/a	$< T(0) >$(Kev.)	$\delta T(0)$(Kev.)
TEXTOR [9][10]	0.77	0.07	0.36	0.30	0.9	0.09
LARS	0.76	0.08	0.39	0.22	0.85	0.13

Table 1. A comparison of TEXTOR data with the LARS simulation.

The simulation appears to give good general agreement, the largest discrepancy being the radial location of the inversion radius. This could be due to the fact that the model does not adequately describe the island region (see Section 4.2).

7 Summary and Discussion

In this paper we have outlined a model for the crash phase of the sawtooth cycle, and derived the set of equations which permits the construction of the unique equilibrium which succeeds the crash. The model has been installed in the '1-1/2 D' resistive evolution code LARS. Unlike the Kadomtsev model, where the mixing radius is determined by reconnection of helical flux, the radius r_m is not specified by the model and could be regarded as a free parameter. However a plausible unique choice for r_m was introduced by requiring relaxation to be restricted to the region in which resistive interchange modes are unstable ($D_R < 0$ as in an RFP). The post-crash core plasma is in a Taylor relaxed state and the entire plasma was allowed to adjust adiabatically so as to provide force balance across the boundary of the relaxed and unrelaxed regions. We generally find $r_m < r_1$, the radius of the $q = 1$ surface. The phenomenon of 'partial' reconnections could be accommodated by a generalisation of the model that permits relaxation only within an annular region surrounding $q = 1$.

The relaxation process is thought of as being initiated by the arrival of the separatrix of an $m/n = 1/1$ island at r_m, the radius where $D_R = 0$. The inboard pressure gradient associated with the separatrix then triggers a collapse of the core pressure and current gradient.

The comparison of the results of this simulation model with the well-diagnosed TEXTOR experimental data shows good quantitative agreement (axial q value, modulation of the axial q etc.). Further details such as the relative positions of the $q = 1$ surface and the inversion radius are also in good agreement.

8 Acknowledgement

The authors thank Dr. J W Connor for discussions. This work was funded jointly by the UK Department of Trade and Industry and Euratom.

9 Figure Captions

Fig. 1. Plot of $q(0)$ after a crash against that before it, for various values of r_m/r_1, based on a cylindrical calculation (see 3.1).

Fig. 2. Resistive evolution of axial q with crash model operative.

Fig. 3. Radial q profile at equally spaced times during an individual ramp.

Fig. 4. Demonstration that the sawtooth acts as an 'antidynamo'. Sawtooth-free resistive evolution is followed until $t = 0.3s.$, and then the crash model is switched on.

Fig. 5. TEXTOR experimental observations of $T(0) - < T(0) >$ during a ramp [10].

Fig. 6. LARS simulation of $T(0) - < T(0) >$ during a ramp with (inset) radial profiles of $T(r)$ at equally spaced times during an individual ramp.

References

[1] Kadomtsev B B, *Sov. J. Plasma Phys.*, **1**, 389, (1975).

[2] Kadomtsev B B, Proc. *Plasma Physics and Controlled Nuclear Fusion Research*, Berchtesgaden, IAEA Vienna, **1**, 555, (1977).

[3] Du Bois M A and Samain A, *Nuclear Fusion*, **20**, 1101, (1980).

[4] Du Bois M A, Pecquet A L and Reverdin C, *Nuclear Fusion*, **23**, 147, (1983).

[5] Soltwisch H, *Rev. Sci. Instrum.*, **59**, 1599, (1988).

[6] O'Rourke J, *Plasma Physics and Controlled Fusion*, **33**, 289, (1991).

[7] Campbell D J *et al*, *Phys. Rev. Lett.*, **57**, 210, (1986).

[8] Wesson J A, Proc. *Theory of Fusion Plasmas*, Varenna, Società Italiana di Fisica, 253, (1987).

[9] Soltwisch H, *Rev. Sci. Instrum.*, **59**, 1599, (1988).

[10] Soltwisch H, Fuchs G, Koslowski H R, Schlüter J, and Waidmann G, in *Proceedings of the 18th. European Conference on Controlled Fusion and Plasma Physics*, Berlin, Vol. 15C, Part II, 17, European Physical Society, (1991).

[11] Taylor J B, *Rev. Mod. Phys.*, **58**, 741, (1986).

[12] Bodin H A B and Newton A A, *Nuclear Fusion*, **20**, 1255, (1980).

[13] Glasser A H, Greene J M and Johnson J L, *Phys. Fluids*, **18**, 875, (1975).

[14] Lutjens H, Bondeson A and Vlad G, *Nuclear Fusion*, **32**, 1625, (1992).

[15] Bondeson A, Vlad G, and Lütjens H, *Phys. Fluids B*, **4**, 1889, (1992).

[16] Ward D J, Theory of fusion plasmas, *Proceedings of the International School of Plasma Physics "Piero Caldirola" Workshop*, Varenna, 295, August 1987.

[17] Fitzpatrick R, Gimblett C G and Hastie R J, *Plasma Physics and Controlled Fusion*, **34**, 161, (1992). See also Corrigenda : Fitzpatrick R, Gimblett C G and Hastie R J, *Plasma Physics and Controlled Fusion*, **34**, 1445, (1992).

[18] Wesson J, *Tokamaks*, Clarendon Press, Oxford, (1987).

[19] Greene J M, Johnson J L and Weimer K E, *Phys. Fluids*, **14**, 671, (1971).

[20] Hastie R J, *Nuclear Fusion*, **29**, 96, (1989).

[21] Bevir M K, Gimblett C G and Miller G, *Phys. Fluids*, **28**, 1826, (1985).

[22] Chu T K, *Nucl. Fusion*, **28**, 1109, (1988).

[23] Fitzpatrick R, Gimblett C G and Hastie R J, *Proceedings of the 20th. EPS Conference on Plasma Physics and Controlled Fusion*, Lisbon, Vol. 17C, Part IV, 1335, European Physical Society, (1993).

[24] Park W, Monticello D and Kuo-Petravic G, *Proceedings of the Workshop on resistive MHD instabilities in Tokamaks with emphasis on the effects of non-circularity and finite beta*, Princeton Plasma Physics Laboratory, November 1988.

[25] Shafranov V D, *Reviews of Plasma Physics* (ed. Leontovich M A) Vol. 2, 103, Consultants Bureau, New York (1966).

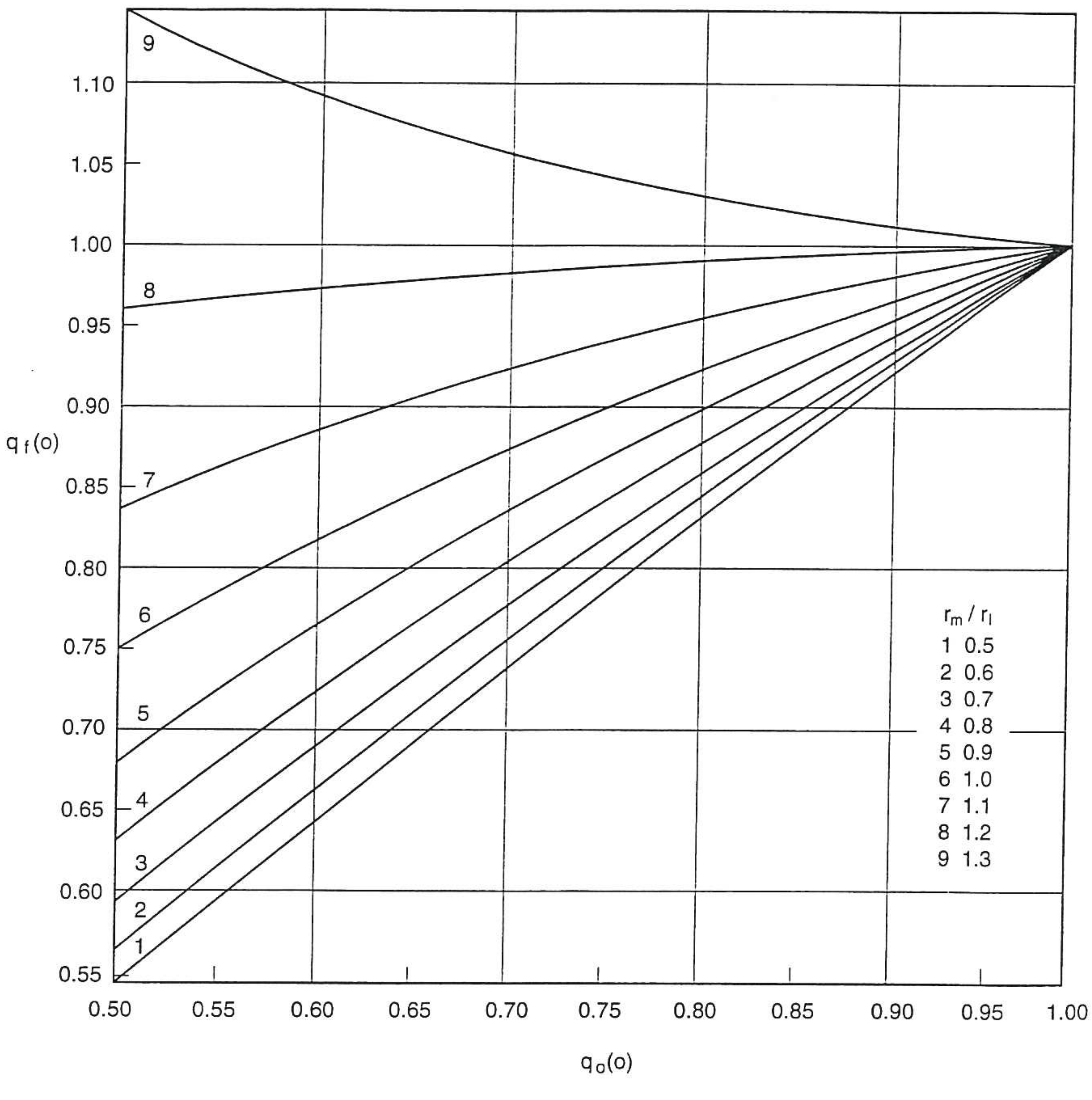

q f(o)
q o(o)
1.10
1.05
1.00
0.95
0.90
0.85
0.80
0.75
0.70
0.65
0.60
0.55
0.50
0.55
0.60
0.65
0.70
0.75
0.80
0.85
0.90
0.95
1.00
1
2
3
4
5
6
7
8
9
r m / r l
1 0.5
2 0.6
3 0.7
4 0.8
5 0.9
6 1.0
7 1.1
8 1.2
9 1.3

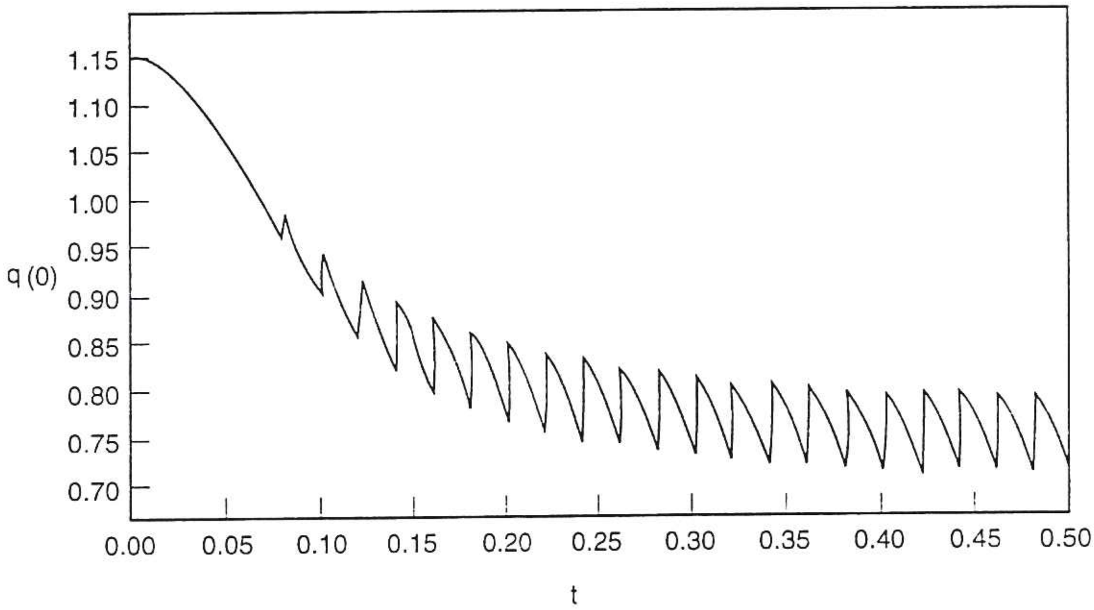

q (0)
1.15
1.10
1.05
1.00
0.95
0.90
0.85
0.80
0.75
0.70
0.00
0.05
0.10
0.15
0.20
0.25
0.30
0.35
0.40
0.45
0.50
t

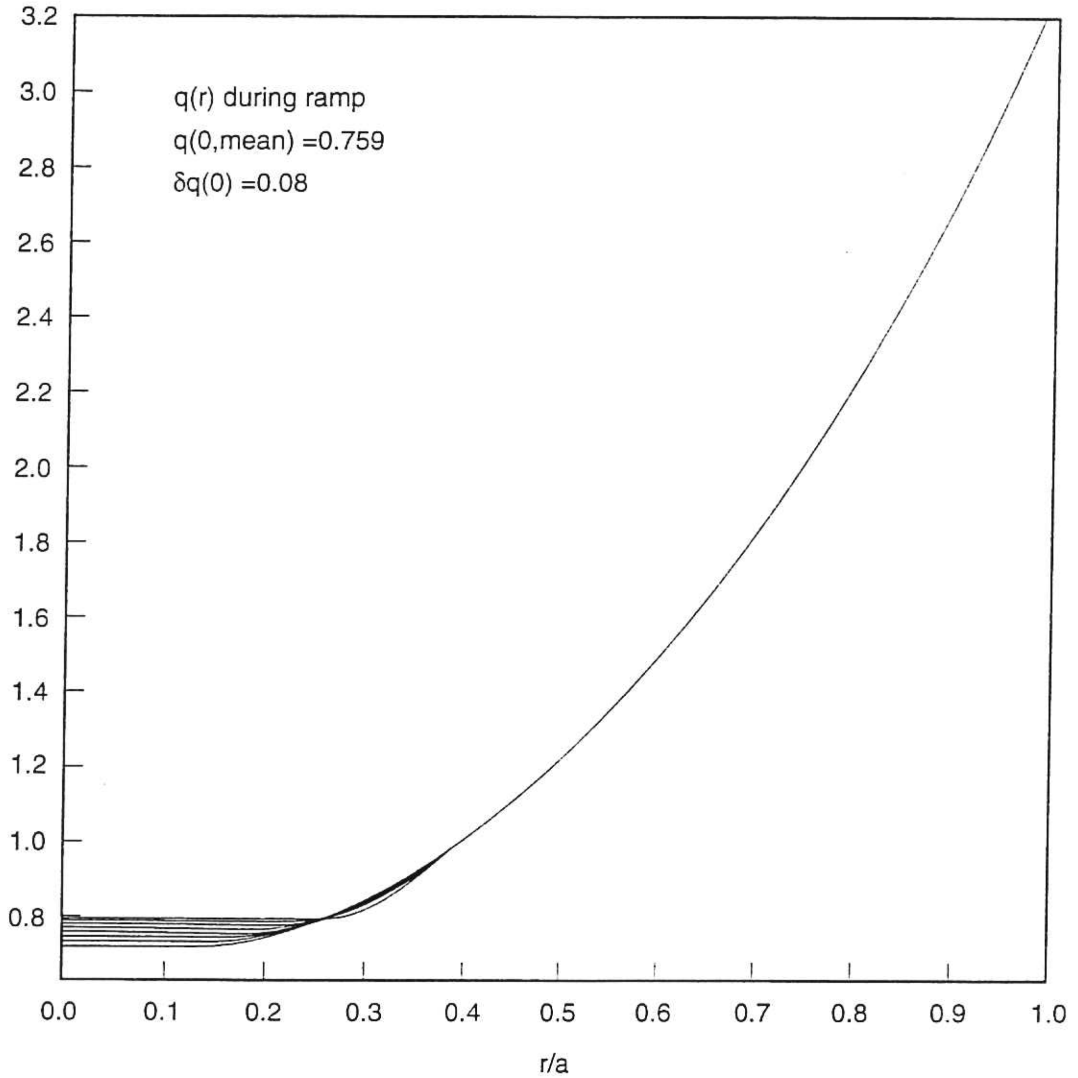

q(r) during ramp
q(0,mean) =0.759
δq(0) =0.08
3.2
3.0
2.8
2.6
2.4
2.2
2.0
1.8
1.6
1.4
1.2
1.0
0.8
0.0
0.1
0.2
0.3
0.4
0.5
0.6
0.7
0.8
0.9
1.0
r/a

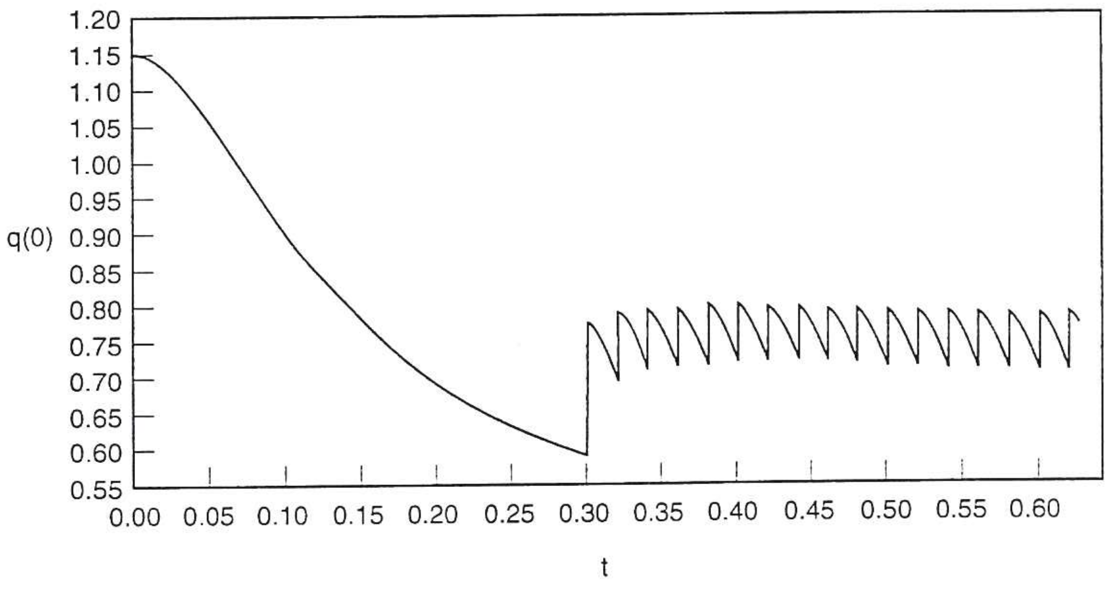

1.20
1.15
1.10
1.05
1.00
0.95
q(0)
0.90
0.85
0.80
0.75
0.70
0.65
0.60
0.55
0.00
0.05
0.10
0.15
0.20
0.25
0.30
0.35
0.40
0.45
0.50
0.55
0.60
t

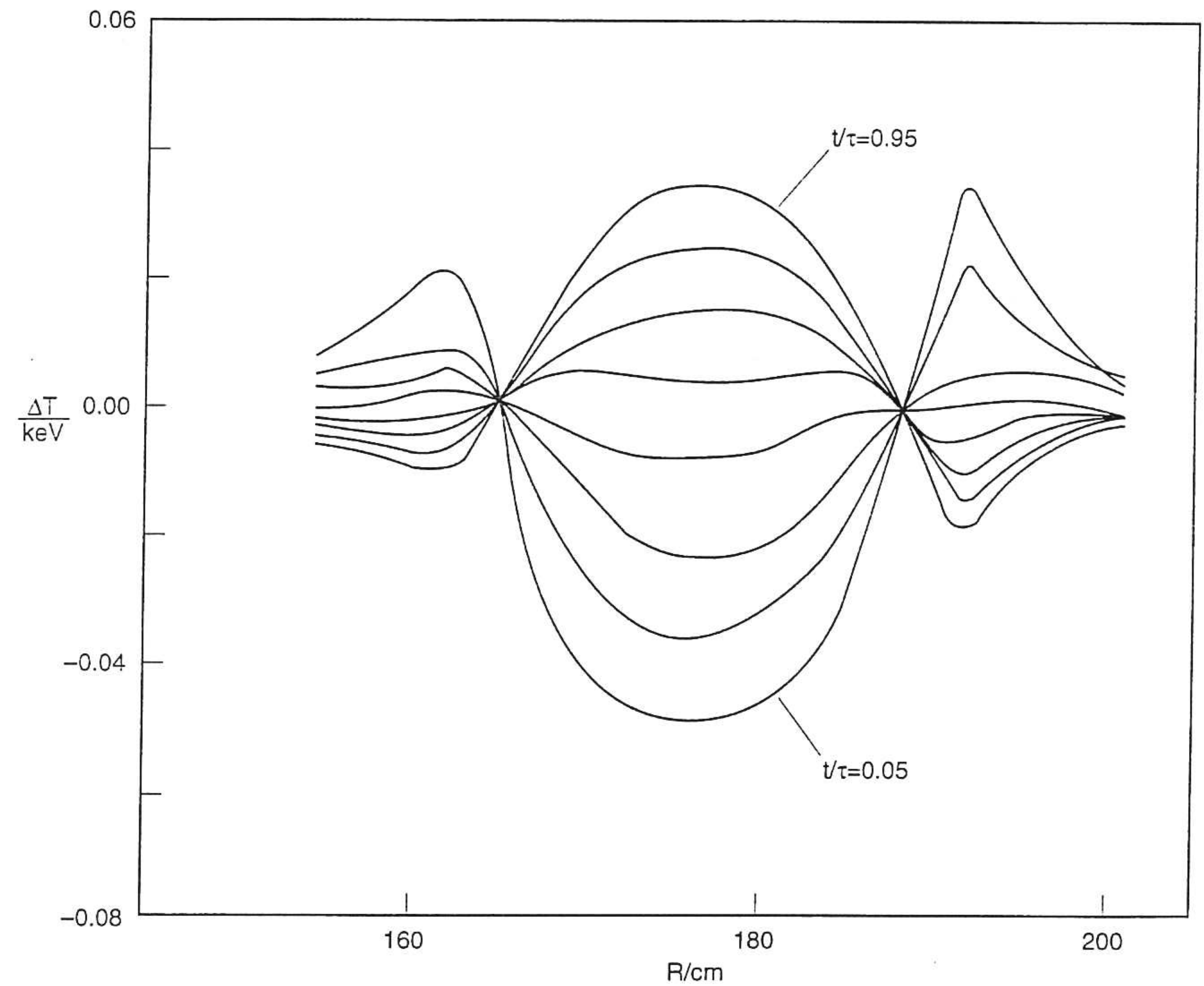

0.06
0.00
−0.04
−0.08
ΔT / keV
t/τ=0.95
t/τ=0.05
160
180
200
R/cm

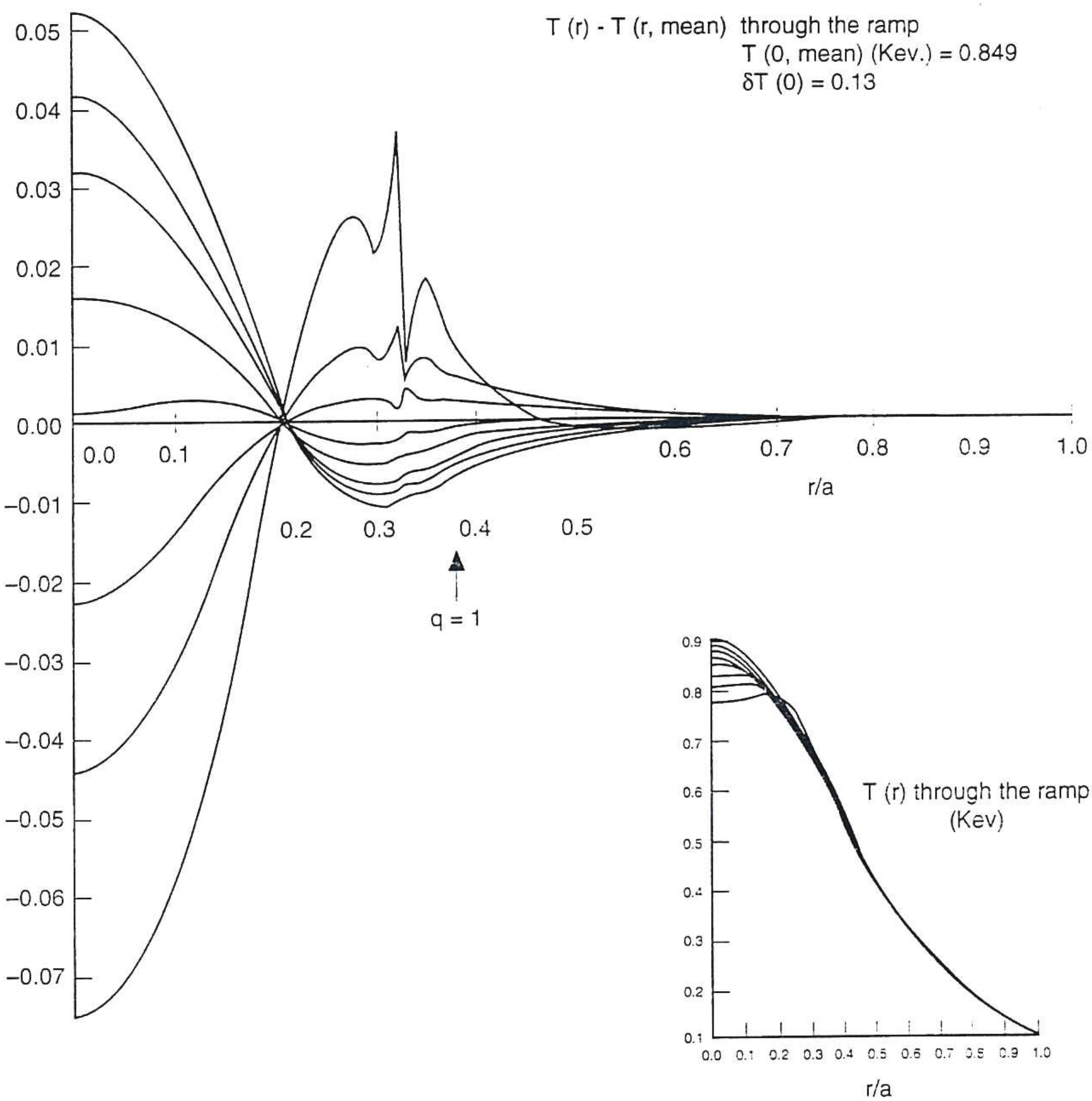
T (r) - T (r, mean) through the ramp
T (0, mean) (Kev.) = 0.849
δT (0) = 0.13
0.05
0.04
0.03
0.02
0.01
0.00
−0.01
−0.02
−0.03
−0.04
−0.05
−0.06
−0.07
0.0 0.1 0.2 0.3 0.4 0.5 0.6 0.7 0.8 0.9 1.0
r/a
q = 1
T (r) through the ramp
(Kev)
0.9
0.8
0.7
0.6
0.5
0.3
0.2
0.1
0.0 0.1 0.2 0.3 0.4 0.5 0.6 0.7 0.9 1.0
r/a